DOI: 10.1093/jnci/djq387 JNCI Journal of the National Cancer Institute Advance Access published October 5, 2010

ARTICLE

Azathioprine-Induced Carcinogenesis in Mice According to *Msh2* Genotype

Alexandra Chalastanis, Virginie Penard-Lacronique, Magali Svrcek, Valérie Defaweux, Nadine Antoine, Olivier Buhard, Sylvie Dumont, Bettina Fabiani, Isabelle Renault, Emmanuel Tubacher, Jean-François Fléjou, Hein te Riele, Alex Duval, Martine Muleris

Manuscript received February 2, 2010; revised August 6, 2010; accepted September 10, 2010.

Correspondence to: Alex Duval, MD, PhD, (e-mail: alex.duval@inserm.fr) and Martine Muleris, PhD, (e-mail: martine.muleris@inserm.fr), Centre de Recherche Saint-Antoine (UMRS 938), Equipe "Instabilité des Microsatellites et Cancers," Hôpital Saint-Antoine, Batiment Kourilsky, 184 rue du Faubourg St Antoine, Paris, France.

Background The thiopurine prodrug azathioprine is used extensively in cancer therapy. Exposure to this drug results in the selection of DNA mismatch repair–deficient cell clones in vitro. It has also been suggested that thiopurine drugs might constitute a risk factor for the emergence of human neoplasms displaying microsatellite instability (MSI) because of deficient DNA mismatch repair.

Methods Azathioprine was administered via drinking water (6–20 mg/kg body weight per day) to mice that were null ($Msh2^{-/-}$; n = 27), heterozygous ($Msh2^{+/-}$; n = 22), or wild type ($Msh2^{WT}$; n = 18) for the DNA mismatch repair gene *Msh2*. Control mice (45 $Msh2^{-/-}$, 38 $Msh2^{+/-}$, and 12 $Msh2^{WT}$) received drinking water lacking azathioprine. The effect of azathioprine on tumorigenesis and survival of the mice was evaluated by Kaplan–Meier curves using log-rank and Gehan–Breslow–Wilcoxon tests. Mouse tumor samples were characterized by histology and immunophenotyping, and their MSI status was determined by polymerase chain reaction analysis of three noncoding microsatellite markers and by immunohistochemistry. *Msh2* status of tumor samples was assessed by loss of heterozygosity analyses and sequencing after reverse transcription–polymerase chain reaction of the entire *Msh2* coding sequence. All statistical tests were two-sided.

Results Most untreated $Msh2^{WT}$ and $Msh2^{+/-}$ mice remained asymptomatic and alive at 250 days of age, whereas azathioprine-treated $Msh2^{WT}$ and $Msh2^{+/-}$ mice developed lymphomas and died prematurely (median survival of 71 and 165 days of age, respectively). Azathioprine-treated $Msh2^{+/-}$ mice developed diffuse lymphomas lacking Msh2 expression and displaying MSI due to somatic inactivation of the functional *Msh2* allele by loss of heterozygosity or mutation. By contrast, azathioprine-treated $Msh2^{WT}$ mice displayed no obvious tumor phenotype, but histological examination showed microscopic splenic foci of neoplastic lymphoid cells that retained Msh2 expression and did not display MSI. Both untreated and azathioprine-treated $Msh2^{-/-}$ mice had a reduced lifespan compared with untreated $Msh2^{WT}$ mice (median survival of 127 and 107 days of age, respectively) and developed lymphomas with MSI.

Conclusion Azathioprine-induced carcinogenesis in mice depends on the number of functional copies of the *Msh2* gene.

J Natl Cancer Inst 2010;102:1–10

Numerous studies have reported an increased risk of cancer among patients who received long-term therapy with drugs, including alkylating agents, topoisomerase inhibitors, and antimetabolites. Because of substantial improvements in drug therapy treatments, patients are now surviving longer and the number of iatrogenic cancers they develop has steadily increased. These cancers likely reflect not only late effects of therapy but also the individual patient's genetic susceptibility, given that individual polymorphic variation in genes involved in carcinogen metabolism and detoxification and DNA repair pathways have been associated with the risk of developing iatrogenic cancers (1). It is therefore important to identify the oncogenic mechanisms responsible for the development of therapy-related malignancies and to understand genetic susceptibility factors that may allow for the identification of individuals at risk for such malignancies.

Among the frequently prescribed antimetabolites are the thiopurines, which comprise azathioprine, 6-mercaptopurine, and 6-thioguanine. Originally used in clinical practice to treat childhood acute lymphoblastic leukemia, 6-mercaptopurine therapy has markedly improved the prognosis of patients with this malignancy (2). The introduction of azathioprine in the 1960s as an immunosuppressant following organ transplantation has also contributed to

CONTEXT AND CAVEATS

Prior knowledge

The thiopurine prodrug azathioprine is used extensively in cancer therapy and as an immunosuppressant in various clinical contexts. However, because exposure to azathioprine results in the selection of DNA mismatch repair–deficient cell clones in vitro, it may constitute a risk factor for the emergence of human neoplasms displaying microsatellite instability.

Study design

Azathioprine was administered to mice that were null (*Msh2*$^{-/-}$), heterozygous (*Msh2*$^{+/-}$), or wild type (*Msh2*^{WT}) for the DNA mismatch repair gene *Msh2* to examine the possible causal association between DNA mismatch repair and thiopurine sensitivity. The effect of azathioprine on tumorigenesis and survival of the mice was compared with that in untreated control mice.

Contribution

Azathioprine-induced carcinogenesis in mice depends on the number of functional copies of the *Msh2* gene.

Implications

Exposure to azathioprine may be an important risk factor for the development of tumors with microsatellite instability, especially for individuals who carry mutations in DNA mismatch repair genes.

Limitations

Whether these observations can be extended to other frequently prescribed immunosuppressants whose actions are independent of DNA mismatch repair is not known.

From the Editors

improvements in patient survival (3). Both drugs are also effective against autoimmune disorders, such as rheumatoid arthritis, autoimmune dermatological diseases, and inflammatory bowel diseases. Although it is now well established that prolonged treatment with thiopurine agents increases the risk of various cancer types, including non-Hodgkin lymphoma, cutaneous squamous cell carcinoma, hepatobiliary carcinoma, and mesenchymal tumors (4,5), the mechanism by which thiopurines contribute to carcinogenesis is not yet understood (6). To date, much of the increased risks of secondary cancers due to thiopurines and other immunosuppressants have been attributed to the effects of immunosuppression per se and to the subsequent involvement of oncogenic viruses (7). In vitro studies have also suggested that defects in the DNA mismatch repair system may be involved in thiopurine sensitivity because exposure of different cell lines to thiopurine agents consistently selects for cells with DNA mismatch repair defects (8–11). DNA mismatch repair is a system for recognizing and repairing the erroneous insertion, deletion, and misincorporation of bases that can arise during DNA replication and recombination, as well as for processing some forms of DNA damage. In eukaryotes, the main protein components of this system are Msh2 and Mlh1. All three thiopurines are inactive prodrugs that are metabolized through a multistep pathway to generate 6-thiodeoxyguanosine, which becomes incorporated into DNA, causing the misincorporation of thymine during DNA synthesis. Recognition and processing of the subsequent mispaired bases by the DNA mismatch repair system results in cell death (12,13). DNA mismatch repair–deficient cells are tolerant to thiopurines because they do not initiate lethal processing of the mispaired bases (14,15). Although DNA mismatch repair deficiency does not by itself cause cells to undergo malignant transformation, it is associated with an increased risk of cancers that exhibit a particular phenotype referred to as microsatellite instability (MSI), which is defined as alterations in the length of short repeated (usually mono- or dinucleotide) sequences of DNA (ie, microsatellites) in tumor tissue relative to normal tissue (16–18).

The accumulation of somatic frameshift mutations defines a so-called mutator pathway that is likely to be oncogenic when it occurs in repeated sequences located within the coding sequence of genes involved in various biological pathways, such as the regulation of cell cycle and/or cell proliferation (eg, *TGFBRII*, *IGFIIR*, *TCF-4*, *AXIN-2*, *PTEN*, *RIZ*), the regulation of apoptosis (eg, *BAX*, *CASP-5*, *BCL-10*, *APAF-1*, *FAS*), or DNA damage signaling and repair (eg, *RAD50*, *BLM*, *MSH3*, *MSH6*, *MBD4*, *MLH3*, *CHK1*, *ATR*). The MSI phenotype characterizes tumors associated with the hereditary nonpolyposis colorectal cancer (HNPCC) syndrome and is also observed in approximately 10%–15% of sporadic colorectal, gastric, and endometrial cancers (19). A high frequency of DNA mismatch repair deficiency has been reported in cancers that arise secondary to chemotherapy, particularly acute myeloid leukemia (AML) and myelodysplastic syndromes, in which the incidence of DNA mismatch repair deficiency is approximately 50%, whereas in de novo AML, it is less than 5% (20). Recent epidemiological studies have reported an association between DNA mismatch repair inactivation and the use of thiopurine regimens in AML and myelodysplastic syndromes that develop in patients treated for autoimmune disorders (5) and in AML and non-Hodgkin lymphomas that develop after organ transplantation (9,21,22). In other clinical contexts such as inflammatory bowel disease, there is no evidence that thiopurines contribute to the development of intestinal neoplasias with MSI (23). To date, there has been no formal in vivo demonstration that these drugs have an effect on MSI-driven oncogenesis.

In this study, we used a mouse model to examine the possible causal association between DNA mismatch repair and thiopurine sensitivity. Azathioprine was administered to mice that were null (*Msh2*$^{-/-}$), heterozygous (*Msh2*$^{+/-}$), or wild type (*Msh2*^{WT}) for the DNA mismatch repair gene *Msh2*. The effect of azathioprine on tumorigenesis and survival of the mice was compared with that in untreated control mice.

Materials and Methods

Mice and Treatment

Mismatch repair–deficient mice carrying a targeted disruption in exon 12 of the *Msh2* gene were described previously (24). *Msh2*$^{+/-}$ mice (129/Ola/FVB) (provided by Professor Hein te Riele) were intercrossed to obtain mice that were null, heterozygous, or wild type for the *Msh2* gene. The genotypes of the mice were determined by using polymerase chain reaction (PCR) analysis, as previously described (25). Groups of mice aged 6 weeks (27 *Msh2*$^{-/-}$ mice, 22 *Msh2*$^{+/-}$ mice, and 18 *Msh2*^{WT} mice) received azathioprine (Imurel 50 mg; GlaxoSmithKline, Marly-le-Roi, France) orally via their drinking water; the estimated dose was 6–20 mg/kg body weight per day, given that a mouse weighs approximately 20–30 g and

drinks approximately 4–8 mL of water per day. This dosage of azathioprine corresponds to a human dose equivalent of 0.5–1.6 mg/kg body weight per day (26), which lies within the range of doses usually prescribed in human therapy (27–31). Control mice (45 *Msh2*$^{-/-}$mice, 38 *Msh2*$^{+/-}$ mice, and 12 *Msh2*^{WT} mice) received water that did not contain azathioprine. All experiments were conducted in accordance with the regulations controlling procedures in live animals in France, after approval of the Ethical Committee for Laboratory Animal Care of the Saint-Antoine research center (Paris, France).

Histopathological and Immunohistochemical Studies

Mice that displayed signs of poor health including breath insufficiency and posterior leg paralysis were killed by cervical dislocation and autopsied. At autopsy, the spleen, liver, and thymus were systematically removed together with other enlarged organs or lymph nodes, and a portion of each type of tissue was stored at –80°C. The remaining portions of tissue were formalin fixed, embedded in paraffin, and sectioned for histological analysis and immunohistochemical staining for Mlh1 and Msh2. For histology, 4-µm sections were stained with hematoxylin–eosin. For Msh2 and Mlh1 immunohistochemistry, 4-µm sections were incubated with mouse monoclonal antibodies against MLH1 (mouse and human cross-reactive clone G168–728; 1:25 dilution; BD Pharmingen, San Diego, CA) and MSH2 (mouse and human cross-reactive clone FE11; 1:25 dilution; Calbiochem, Cambridge, MA) as previously described (32), followed by incubation with the appropriate secondary antibodies (Trekkie biotinylated mouse link and trekavidin–HRP label; Biocare, Paris, France). Stromal and normal lymphocytes that were present in the section served as the control for positive staining. For immunophenotyping, 6-µm thick acetone-fixed frozen sections of spleen were incubated with a rat monoclonal antibody against mouse CD45, which recognizes hematopoietic cells (clone 30-F11; 1:50 dilution; BD Pharmingen), a rabbit monoclonal antibody against CD3, which recognizes T cells (mouse and human cross-reactive clone sp7; 1:100 dilution; Interchim, Montluçon, France), and a biotinylated rat monoclonal antibody against mouse CD19, which recognizes B cells (clone 6D5; 1:100 dilution; Abcam, Paris, France). Sections were then incubated with the following horseradish peroxidase–conjugated secondary antibodies: rabbit anti-rat immunoglobulin G (1:250 dilution; Abcam), amplification system anti-rabbit (Ready-to-use Envision+ system; Dako, Trappes, France), and horseradish peroxidase–streptavidin conjugate (1:500 dilution; Zymed, Invitrogen, Cergy Pontoise, France), respectively. Peroxidase activity (ie, bound antibody) was detected with the use of a DAB+ kit (Dako).

Microdissection of Mouse Tumor Tissue Sections

The tumor cell component from two azathioprine-treated *Msh2*^{WT} mice selected at random was collected from 10 hematoxylin- and eosin-stained 7-µm tissue sections per mouse with the use of a laser-capture microdissection system (PALM Laser; Zeiss, Le Pecq, France) and used for DNA extraction.

PCR-Based *Msh2* Genotyping of Normal and Tumor DNA

Normal DNA (from mouse tail) and tumor DNA were extracted with the use of a QIAamp DNA extraction kit (Qiagen, Courtaboeuf, France) according to the manufacturer's instructions. *Msh2* genotype analysis was performed as previously described (25) by using a three-primer allele-specific PCR assay in which the wild-type and inactivated *Msh2* alleles generated PCR products of 164 and 194 bp, respectively. Briefly, PCR was performed using Taq DNA Polymerase kit (Qiagen) with 0.5 mM $MgCl_2$, 0.2 mM dNTP mix, and 0.5pmol/µL of each primer (primers are detailed in Supplementary Table 1, available online). PCR conditions were 94°C for 5 minutes followed by 35 cycles of 94°C for 30 seconds, 60°C for 30 seconds, and 72°C for 30 seconds, and a final extension at 72°C for 7 minutes. The PCR products were resolved on agarose gels. To assess loss of heterozygosity of the *Msh2* allele, quantitative densitometry scanning of the DNA bands on a 4% agarose gel was carried out with the use of GeneTools software (version 4.01; Syngene, Saint Quentin en Yvelines, France). Allelic loss was calculated using the following normalized allelic imbalance ratio (WT tumor to D tumor)/(WT normal to D normal), where WT and D correspond to the wild-type and disrupted alleles, respectively. An allelic imbalance ratio less than 0.6 was considered indicative of loss of heterozygosity based on the observation that some tumors contained an estimated 40% of normal stromal cells interspersed among the tumor cells.

Msh2 Gene Sequencing

Reverse transcription–PCR was used to generate eight overlapping DNA fragments that covered the entire *Msh2* coding sequence. Total RNA was extracted from nine mouse tissue samples—four tumor sites and the corresponding normal tissue from mouse 36 (an azathioprine-treated *Msh2*$^{+/-}$ mouse that did not show loss of heterozygosity of the *Msh2* allele), and tumor tissues from four other mice for controls (three azathioprine-treated *Msh2*$^{+/-}$ mice and one untreated *Msh2*$^{-/-}$ mouse)—with the use of an RNeasy extraction kit (Qiagen) according to the manufacturer's instructions. For reverse transcription, we used 700 µg of RNA and murine leukemia virus reverse transcriptase and oligo dT from a GeneAmp RNA PCR kit (Perkin Elmer, Courtaboeuf, France). PCR was performed with the use of a HotStarTaq DNA Polymerase kit (Qiagen) with 3 mM $MgCl_2$ and 0.3 µM of each primer (primers are detailed in Supplementary Table 1, available online). The PCR profile was 95°C for 15 minutes followed by 35 cycles of 95°C for 30 seconds, 63°C for 30 seconds, and 72°C for 1 minute. Sequencing was done by a linear amplification with the use of a Big Dye Terminator v1.1 Cycle sequencing kit (Applera, Courtaboeuf, France) according to the manufacturer's instructions. PCR products were analyzed on an ABI PRISM 3100 Genetic Analyzer (Applera). Identified DNA sequence variants were confirmed by sequencing both DNA strands.

Analysis of MSI

We used three noncoding mononucleotide repeats (all on chromosome 1) to determine tumor MSI status: A22, A24, and T40. PCR reactions were performed using DNA (50 ng) isolated from tumor and normal tissues from the same mouse, GoTaq DNA Polymerase (Promega, Charbonnieres, France), 1.5 mM $MgCl_2$, and 0.3 µM of each primer (Supplementary Table 1, available online). The PCR profile was 94°C for 5 minutes followed by 35 cycles of 94°C for 30 seconds, 50°C (for A22 and A24) or 54°C (for T40) for 30

seconds and 72°C for 30 seconds, with final extension at 72°C for 7 minutes. Amplified products were resolved on denaturing gels run in an ABI PRISM 3100 Genetic Analyzer and analyzed using Genescan 3.7 and Genotyper 2.1 software programs (Applera). We compared the predominant allele size observed in the tumor with that observed in normal tissue from the same mouse (ie, 190, 70, and 122 for markers A22, A24, and T40, respectively). Tumors were scored as MSI positive if the length of at least one marker in tumor DNA differed from that in normal tissue DNA.

Mutation Analysis of Target Genes for MSI

To confirm the role of MSI as an active oncogenic process in lymphoma cells, we screened for frameshift mutations in coding microsatellites of cancer-related genes. Most coding microsatellite sequences that are contained within human genes are not conserved in the murine genome. We therefore constructed an in silico database by querying GenBank (October 2007) for murine genes that contain coding microsatellite sequences greater than seven nucleotides in length (available on request from the authors). From this database, we selected nine genes with involvement in tumorigenesis that were possible targets for mutation by MSI: *Sdccag1*, *Casc3*, *Kit*, *Casc5*, *Rasal2*, *FasL*, *Tcf7l2*, *Apc*, and *Akt3*. Only one of these genes, *Tcf7l2* (also known as *Tcf-4*, the main effector of Wnt and Wingless signaling), was known to be mutated in a conserved microsatellite sequence in human colorectal tumors with MSI (33). Screening for mutation was performed by PCR using tumor or corresponding normal DNA (50 ng), primers specific for each gene (at 0.3 μM; Supplementary Table 1, available online), and a Taq DNA Polymerase kit (Qiagen). The PCR profile was 94°C for 4 minutes, followed by 35 cycles of 94°C for 30 seconds, 60°C for 30 seconds, and 72°C for 1 minute, with a final extension at 72°C for 7 minutes. Tumors were scored as mutated if the length of the predominant allele in tumor DNA differed from that in normal tissue DNA.

Generation of Kaplan–Meier Survival Curves and Statistical Analysis

The health of the mice was examined daily. Mice that presented with signs of poor health were killed by cervical dislocation according to the recommendations of our Ethical Committee. In our experience, these signs are due to lymphomagenesis (34,35) and precede the time of death by a couple of days. The time of death was recorded for each mouse that was found dead or had been killed. Kaplan–Meier survival curves were generated with the use of Graphpad Prism software (version 4; Graphpad, Inc, San Diego, CA). Comparisons of median survivals were performed using log-rank and Gehan–Breslow–Wilcoxon tests. Comparisons of the mean number of tumors in $Msh2^{-/-}$ and treated $Msh2^{+/-}$ mice were performed using the Student *t* test. All statistical tests were two-sided.

Results

Effect of Azathioprine on Mouse Tumorigenesis and Survival According to *Msh2* Genotype

Previous studies demonstrated that heterozygous $Msh2^{+/-}$ mice have a normal lifespan, whereas most $Msh2^{-/-}$ mice spontaneously develop diffuse aggressive lymphomas and succumb to these by 6–8 months of age (34,35). In agreement with these findings, we observed that most (82%) of the untreated $Msh2^{+/-}$ mice remained free of disease, whereas all untreated $Msh2^{-/-}$ mice were dead by age 200 days (Figure 1). $Msh2^{+/-}$ and $Msh2^{WT}$ mice that received azathioprine via their drinking water showed statistically significantly shorter survival compared with the respective untreated mice: All treated mice were dead by age 250 days (log-rank test: $P < .001$; Gehan–Breslow–Wilcoxon test: $P < .001$). However, azathioprine-treated $Msh2^{+/-}$ mice had statistically significantly longer median survival compared with azathioprine-treated $Msh2^{WT}$ mice (165 vs 71 days, difference = 94 days, 95% confidence interval [CI] = 55 to 133 days; $P < .001$ [Gehan–Breslow–Wilcoxon test]; Figure 1). Conversely, azathioprine-treated $Msh2^{-/-}$ mice had slightly longer median survival compared with untreated $Msh2^{-/-}$ mice (127 vs 107 days, difference = 20 days, 95% CI = –9 to 49 days, $P = .03$ log-rank test; $P = .01$ [Gehan–Breslow–Wilcoxon test]; Figure 1).

All azathioprine-treated $Msh2^{-/-}$ mice (n = 15), untreated $Msh2^{-/-}$ mice (n = 10), and azathioprine-treated $Msh2^{+/-}$ mice (n = 8) that were autopsied were found to have developed a tumoral phenotype that was characterized by abnormal enlargement of the thymus, spleen, and liver, sometimes in association with adenomegaly. Histological examination of all tumor masses revealed massive infiltration of organs by medium-to-large lymphoid cells (Figure 2, A and Supplementary Table 2 [available online]). Of note, the mean number of macroscopic tumor sites did not differ statistically significantly between $Msh2^{-/-}$ mice (treated and untreated combined) and treated $Msh2^{+/-}$ mice (2 vs 3 sites, difference = 1 site, 95% CI = 0.94 to 1.06 sites; $P = .13$ [Student *t* test]) (Supplementary Table 2, available online). An identical syndrome was observed in one untreated $Msh2^{+/-}$ mouse. By contrast, none of the 11 azathioprine-treated $Msh2^{WT}$ mice that were analyzed displayed obvious enlargement of organs; however, histological examination of these mice confirmed, in most instances (nine of 11 mice), the presence of microscopic foci comprising medium-to-large neoplastic lymphoid cells that were restricted to the spleen area located under the capsule (Figure 2, A). There were no histological or immunophenotypical differences between azathioprine-induced and spontaneous lymphomas in mice with any *Msh2* genotype (Figure 2, B and Supplementary Table 3 [available online]). All but one of the lymphomas was of B-cell origin (ie, CD45 positive, CD19 positive, and CD3 negative); one tumor sample from an azathioprine-treated $Msh2^{+/-}$ mouse was of T-cell origin (ie, CD45 positive, CD19 negative, and CD3 positive).

MSI Status of Azathioprine-Induced Lymphomas in $Msh2^{+/-}$ and $Msh2^{WT}$ Mice

We next examined tumor DNA for three noncoding microsatellite markers to determine whether the tumors that developed in azathioprine-treated $Msh2^{+/-}$ and $Msh2^{WT}$ mice differed in terms of MSI status. Most of tumor DNA samples from $Msh2^{-/-}$ mice displayed MSI (defined as a change in the length of one or more microsatellite loci compared with normal tissue DNA from the same mouse) (Figure 3, A). In all, 43 of 50 lymphomas from 25 $Msh2^{-/-}$ mice (including 15 of 18 lymphomas from 10 untreated mice and 28 of 32 lymphomas from 15 azathioprine-treated mice) displayed MSI demonstrating a sensitivity of 86% (95% CI = 73%

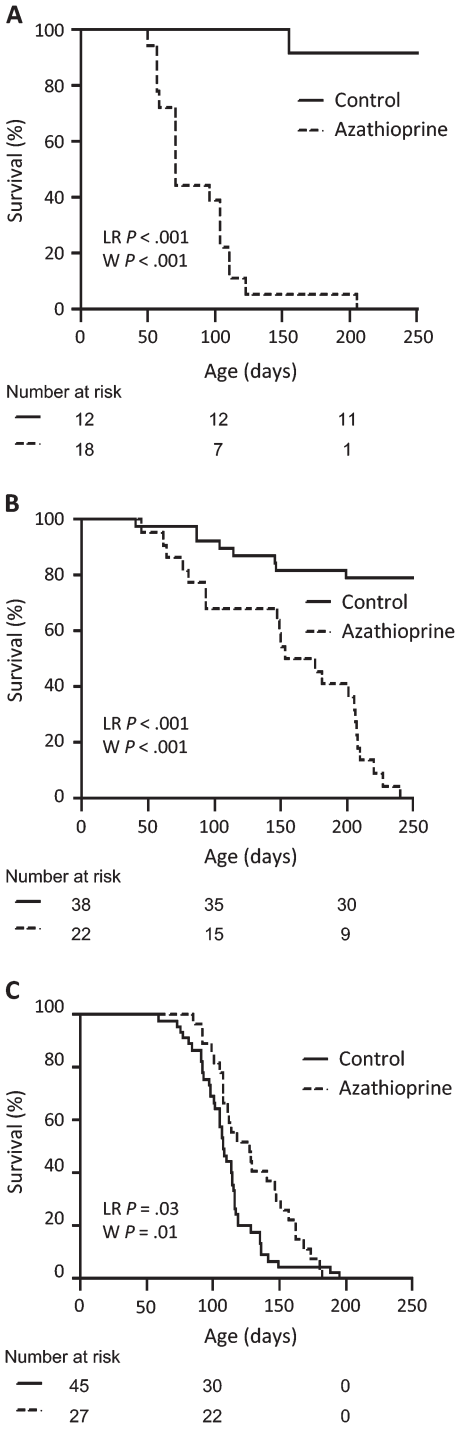

Figure 1. Kaplan–Meier survival analysis of azathioprine-treated and untreated mice. **A**) *Msh2*^{WT} mice. **B**) *Msh2*$^{+/-}$ mice. **C**) *Msh2*$^{-/-}$ mice. All *P* values are two-sided. W = Gehan–Breslow–Wilcoxon test; LR = log-rank test.

to 94%) for our panel of markers (Supplementary Table 2, available online). Of interest, 22 (92%) of 24 tumors from eight azathioprine-treated *Msh2*$^{+/-}$ mice were also scored as MSI (Figure 3, A and Supplementary Table 2 [available online]). The single untreated *Msh2*$^{+/-}$ mouse that developed a spontaneous tumor syndrome had five lymphoma sites, all of which displayed the MSI phenotype. As a control, normal (mouse tail) DNA from *Msh2*^{WT} and *Msh2*$^{+/-}$ mice did not exhibit change in the length of microsatellite loci, and alterations in the allelic size of the three markers were only occasionally observed in normal DNA from *Msh2*$^{-/-}$ mice (Figure 3, A). By contrast, tumor cells isolated using laser microdissection from splenic microproliferations of two azathioprine-treated *Msh2*^{WT} mice did not display MSI when analyzed with the microsatellite markers (Figure 3, A and Supplementary Table 2 [available online]).

Msh2 Expression in Lymphoma Cells From Azathioprine-Treated *Msh2*$^{+/-}$ Mice and *Msh2*^{WT} Mice

A total of 16 of the 24 tumors from azathioprine-treated *Msh2*$^{+/-}$ mice for which there was remaining tissue available were analyzed for Msh2 expression by immunohistochemistry. All 16 tumor samples showed no staining of the tumor cells, indicating the loss of Msh2 expression in lymphoma cells from azathioprine-treated *Msh2*$^{+/-}$ mice (Figure 3, B and Supplementary Table 2 [available online]). PCR-based genotyping that was performed on all tumors from both azathioprine-treated (n = 24) and untreated *Msh2*$^{+/-}$ mice (n = 5) showed that in most of these tumors (25 [86%] of 29), loss of Msh2 expression in lymphoma cells from *Msh2*$^{+/-}$ mice resulted from somatic loss of the remaining wild-type *Msh2* allele through loss of heterozygosity (Figure 4, A and B). In one *Msh2*$^{+/-}$ mouse that was treated with azathioprine, we identified a variant form of *Msh2* that contained a G to T transversion at codon 2074 in exon 13, which resulted in the substitution of glycine to tryptophan at amino acid 692 (Figure 4, B). This mutation was present in the DNA from the four primary tumor sites in this mouse but absent from the normal DNA. Although this missense mutation has not been previously reported in HNPCC patients, it is important to note that it occurs in a well-conserved region of the gene and that the substitution of glycine to tryptophan at amino acid 692 has been reported in a Portuguese HNPCC family (36), which suggest the possible pathogenicity of this variant. Moreover, an in silico analysis of the function of the mutated protein (performed on the *PolyPhen*: prediction of functional effects of human nsSNP website; http://genetics.bwh.harvard.edu/pph/) predicted that the mutation was likely to disrupt the function of the Msh2 protein (data not shown).

By contrast, immunohistochemical analysis revealed that tumor samples from the nine azathioprine-treated *Msh2*^{WT} mice that displayed microscopic foci of neoplastic lymphoid cells retained the expression of the two DNA mismatch repair genes, *Msh2* (Figure 3, B and Supplementary Table 2 [available online]) and *Mlh1* (data not shown), indicating that the carcinogenic process in these mice was unlikely to be due to inactivation of DNA mismatch repair.

Oncogenic Pathway in Lymphoma Cells with MSI from Control and Azathioprine-Treated Mice

Finally, to confirm the role of MSI as an active oncogenic process in lymphoma cells from mice in this study, we investigated whether the instability observed in noncoding microsatellites of DNA mismatch repair–deficient lymphoma cells was accompanied by somatic mutations in the coding microsatellites of cancer-related genes, as was previously reported (37). We screened for frameshift mutations in coding microsatellites in nine candidate genes (*Sdccag1*, *Casc3*, *Kit*, *Casc5*, *Rasal2*, *FasL*, *Tcf7l2*, *Apc*, and *Akt3*) with putative roles in carcinogenesis. Screening for mutation was performed by

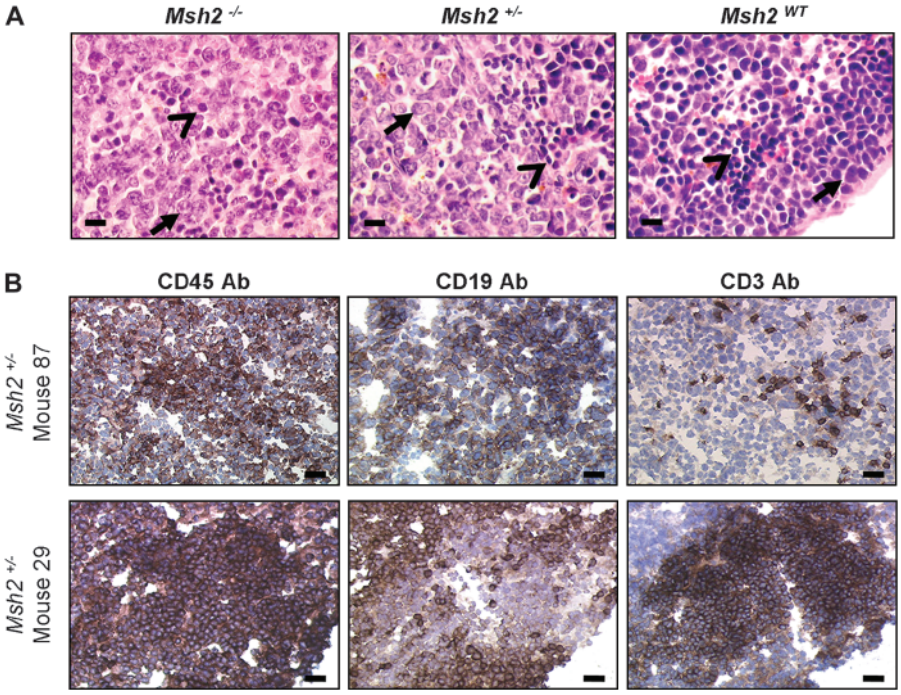

Figure 2. Histological and immunohistochemical characterization of murine lymphomas. **A**) Hematoxylin–eosin staining of splenic lymphoma from azathioprine-treated *Msh2*$^{-/-}$, *Msh2*$^{+/-}$, and *Msh2*^{WT} mice. **Arrows** indicate tumor cells; **arrowheads** indicate normal lymphocytes. **B**) Immunohistochemistry of spleen tissue cryosections from two azathioprine-treated *Msh2*$^{+/-}$ mice. Adjacent sections of spleen from each mouse were stained with antibodies against CD45 to identify hematopoietic cells, against CD3 to identify T cells, or against CD19 to identify B cells. **Brown** indicates positive staining. Scale bars = 30 μm.

comparing the predominant allele size of PCR product in tumor and corresponding normal DNA in a representative sample of tumors that displayed MSI (ie, 61 tumor samples from six azathioprine-treated *Msh2*$^{+/-}$ mice, one *Msh2*$^{+/-}$ untreated mouse, 14 azathioprine-treated *Msh2*$^{-/-}$ mice, and four untreated *Msh2*$^{-/-}$ mice) (Figure 3, C). Frameshift mutations were found in eight of the target genes, of which the *Sdccag1* (serologically defined colon cancer antigen 1) and *Casc3* (cancer susceptibility candidate 3) genes were mutated at relatively high frequencies in these tumors (58% and 21%, respectively; Figure 3, C). The mutation frequency for each of the nine target genes was similar in spontaneous and azathioprine-induced lymphomas (data not shown). The relatively high frequencies of frameshift mutations in *Sdccag1* and *Casc3* pointed to an active oncogenic MSI pathway in lymphomas from *Msh2*$^{-/-}$ and *Msh2*$^{+/-}$ mice. The human *SDCCAG1* homolog has been identified as a tumor suppressor in non–small cell lung cancer cell lines (38,39). The Casc3 protein is a component of a splicing-dependent multi-protein junction complex that marks the position of the exon–exon junction in mature mRNA (40), thereby influencing downstream gene expression processes including mRNA splicing, nuclear mRNA export, subcellular mRNA localization, translation efficiency, and nonsense-mediated mRNA decay. Casc3 could then play a role in MSI-driven carcinogenesis, given that numerous frameshift mutation–derived mRNAs are processed by the nonsense-mediated mRNA decay machinery in MSI tumors (41,42). It is noteworthy that in a given mouse, some tumor locations displayed a mutation in *Sdccag1* or *Casc3* genes, whereas other tumor sites did not, suggesting that the mutations occurred as independent molecular events during disease progression (Figure 3, D).

Discussion

Thiopurines are effective anticancer agents and immunosuppressants in a variety of clinical conditions. However, they have been reported to be associated with an increased incidence of secondary tumors (6). It is therefore important to identify the oncogenic mechanisms responsible for the development of iatrogenic neoplasms because such information could allow the identification of patients who may be at risk of developing tumors when treated with these drugs. For this purpose, we investigated whether a murine model could be used to examine the causal involvement of DNA mismatch repair in thiopurine sensitivity. We administered azathioprine to mice that were wild type or inactivated in one or both copies of the DNA mismatch repair gene *Msh2*. The dosage of azathioprine used in our mouse model corresponds to a human dose equivalent of 0.5–1.6 mg/kg body weight per day (26) and lies within the range usually prescribed in human therapy. As a mutagen and immunosuppressant, azathioprine was expected to induce tumor formation in mice, which turned out to be the case. However, it is interesting that we also found that the oncogenic pathway, the survival, and the tumoral phenotype of azathioprine-treated mice were influenced by their *Msh2* status. Briefly, we observed that azathioprine-treated *Msh2*^{WT} and *Msh2*$^{+/-}$ mice developed lymphomas and died prematurely (median survival of 71 vs 165 days of age, respectively) compared with the respective untreated mice that mostly were alive at 250 days of age. However, we demonstrated that *Msh2*$^{+/-}$ mice developed diffuse lymphomas that lacked Msh2 expression and displayed MSI at both noncoding and coding microsatellite sequences because of somatic inactivation of the remaining functional *Msh2* allele in tumor cells. By contrast, *Msh2*^{WT} mice presented with splenic microscopic foci of neoplastic lymphoid cells that retained both Msh2 and Mlh1 expression and did not display MSI. Both untreated and azathioprine-treated *Msh2*$^{-/-}$ mice developed diffuse MSI lymphomas as expected, but surprisingly, the former had slightly longer median survival (median survival of 127 vs 107 days of age, respectively). Our data thus clearly demonstrate the ability of azathioprine to trigger carcinogenesis through an MSI-driven process in vivo.

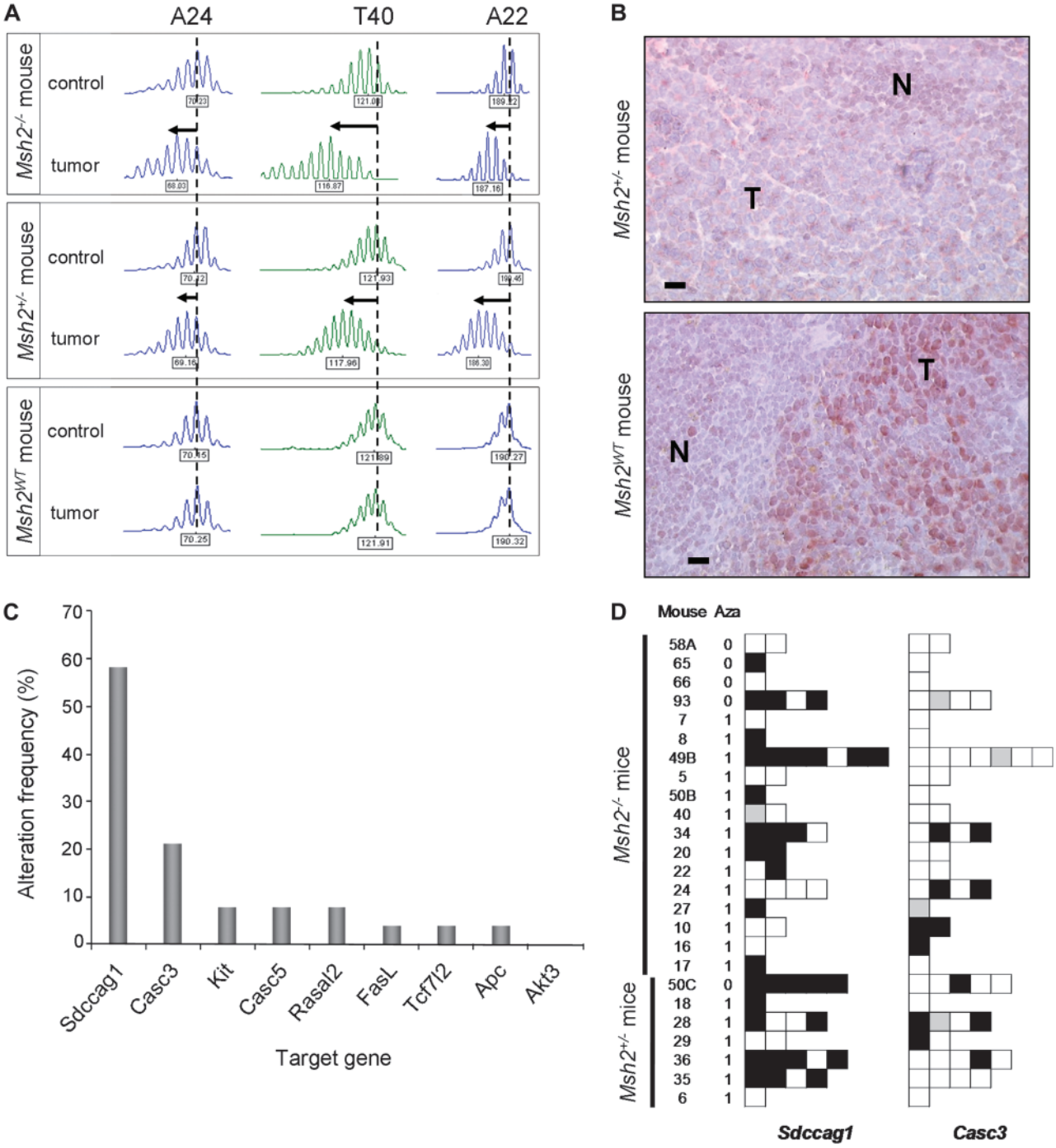

Figure 3. Msh2 expression and instability analysis in noncoding and coding microsatellites in lymphomas from azathioprine-treated mice. **A**) Allelic profiles of noncoding microsatellite markers A22, A24, and T40 in normal (control) and tumor tissues from three mice. Shown are representative profiles displaying shorter alleles (**arrows**) for the three markers in tumor DNA compared with the corresponding normal tissue DNA in an *Msh2*$^{-/-}$ mouse and an *Msh2*$^{+/-}$ mouse. In the representative profile for the *Msh2*^{WT} mice, the sizes of the microsatellites did not differ between tumor and normal tissue. Length of the predominant allele (bp) is indicated in a box below each profile. **Dashed vertical lines** indicate the predominant allele size observed in control DNA from all *Msh2*$^{+/-}$ and *Msh2*^{WT} mice analyzed (reference value). Note that the size of the predominant allele of markers T40 and A22 differed from this reference value in the normal DNA from the *Msh2*$^{-/-}$ mouse. **B**) Immunohistochemical analysis of Msh2 expression in lymphomas. Shown are representative images of staining of tumor sections from an *Msh2*$^{+/-}$ mouse and an *Msh2*^{WT} mouse with an Msh2 antibody. Tumor cells were not stained in the *Msh2*$^{+/-}$ mice, whereas they stained positively in the *Msh2*^{WT} mice. Normal lymphocytes showed a less pronounced Msh2 staining due to their lower proliferation rate. **Red** indicates positive staining. T = medium-to-large neoplastic lymphoid cells; N = normal lymphocytes. Scale bar = 30 μm. **C**) Mutation analysis of target genes for microsatellite instability (MSI). Analysis was performed by comparing the predominant allele size of the coding microsatellite in tumor DNA and corresponding normal tissue DNA. Two genes displayed frameshift mutations at relatively high frequencies, *Sdccag1* and *Casc3*, pointing to an active oncogenic MSI pathway in lymphomas from *Msh2*$^{-/-}$ and *Msh2*$^{+/-}$ mice. **D**) Details of the *Sdccag1* and *Casc3* mutation status in individual tumors from *Msh2*$^{-/-}$ and *Msh2*$^{+/-}$ mice. Each row corresponds to a single mouse, each square represents a tumor site in that mouse, numbers correspond to mouse number, mice received azathioprine (Aza) treatment (1) or not (0). Black = mutated; white = wild type; gray = analysis not informative.

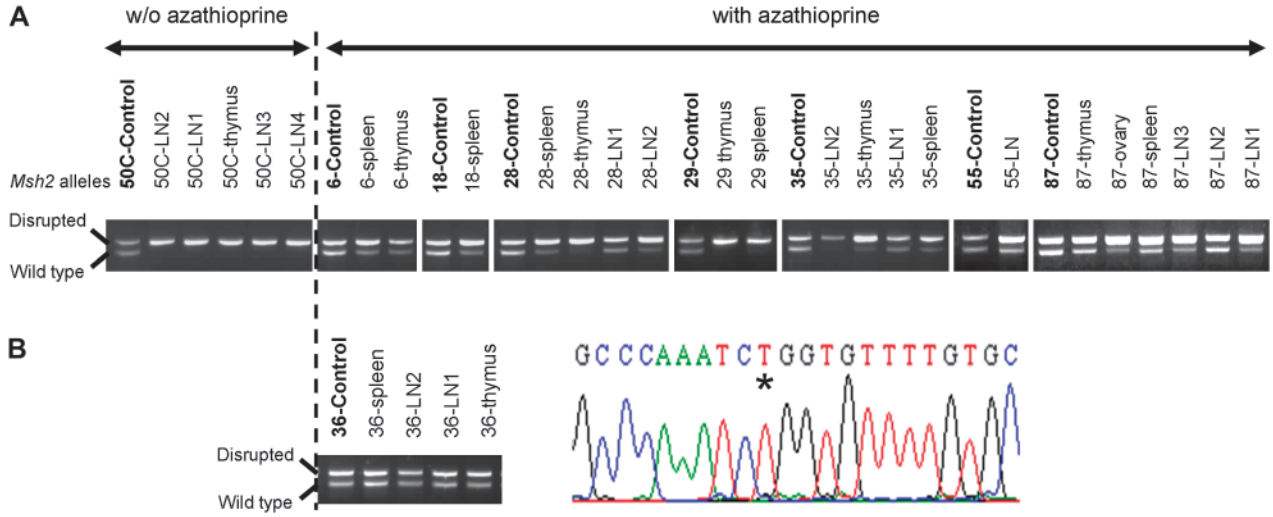

Figure 4. Loss of heterozygosity analyses and sequencing of the *Msh2* coding sequence in tumor tissues from *Msh2*$^{+/-}$ mice. DNA bands on the gel electrophoresis after polymerase chain reaction–based genotyping are shown for all tumor samples from nine *Msh2*$^{+/-}$ mice (numbers correspond to mouse number). Some tumor sites showed complete loss of signal for the wild-type allele, whereas other sites showed residual signal corresponding to contamination from non–tumor cell DNA. The intensity ratio of the two allelic bands (wild type and disrupted) in tumor DNA relative to that obtained in normal (control) DNA was calculated and a ratio of 0.6 or less corresponding to a reduction of intensity of at least 40% in tumor DNA was used to score loss of heterozygosity. **A**) Loss of the wild-type *Msh2* allele in all tumor sites for eight mice. LN = lymph node. **B**) Mutation of the wild-type *Msh2* allele in tumor sites from mouse 36. In the single mouse in which the wild-type allele was retained at all four sites examined (**left**), a G to T transversion (**asterisk**) in exon 13 of the *Msh2* gene was detected by sequencing after reverse transcription—polymerase chain reaction analysis of the entire *Msh2* coding sequence (**right**).

To date, two mechanisms have been reported to underlie the cytotoxicity of azathioprine. First, azathioprine-induced purine starvation slows the rate of cell division, especially in lymphocytes, which, unlike other cell types, cannot use the salvage pathway of purine synthesis (43–45). Importantly, this effect has not been demonstrated to be dependent on *Msh2* status. Second, DNA mismatch repair–dependent signaling of azathioprine-induced DNA damage results in apoptosis in DNA mismatch repair–proficient cells (12,13). By contrast, DNA mismatch repair–deficient cells display thiopurine tolerance and are therefore able to escape cell death when exposed to azathioprine (14,15) and subsequently undergo neoplastic cell transformation through the accumulation of genetic mutations caused by MSI. Moreover, the MSI-driven oncogenic pathway has been shown previously to favor the emergence of a tumor phenotype in mice that is characterized by an enlarged thymus, spleen, and liver and which leads *Msh2*$^{-/-}$ mice to die from diffuse aggressive lymphomas (34,35). Taking all these elements into consideration, we propose the following explanations to account for the various oncogenic pathways, survival, and tumoral phenotypes observed in azathioprine-treated mice with different *Msh2* status. First, untreated *Msh2*$^{-/-}$ mice exhibited the characteristic development of MSI lymphomas, which were ultimately responsible for their death (see above). Azathioprine-treated *Msh2*$^{-/-}$ mice displayed the same tumor phenotype as untreated mice, but had slightly longer survival, which may reflect reduced *Msh2*$^{-/-}$ lymphocyte proliferation due to purine starvation resulting from azathioprine treatment. Second, azathioprine-treated *Msh2*$^{+/-}$ mice were similar to both treated and untreated *Msh2*$^{-/-}$ mice with respect to tumor phenotype, histology, and MSI status of lymphoma cells. A reasonable explanation for this finding is that like (treated and untreated) *Msh2*$^{-/-}$ mice, azathioprine-treated *Msh2*$^{+/-}$ mice died from lymphomas that had MSI and an active oncogenic mutator pathway. The longer median survival of azathioprine-treated *Msh2*$^{+/-}$ mice compared with azathioprine-treated *Msh2*$^{-/-}$ mice (165 vs 127 days) may be due to the time required for somatic inactivation of the remaining functional *Msh2* allele in the *Msh2*$^{+/-}$ mice, in accordance with the Knudson two-hit model (46). Finally, azathioprine-treated *Msh2*^{WT} mice exhibited a distinct tumor phenotype but no enlarged organs. Histological examination revealed microscopic foci of lymphoma cells expressing Msh2 and Mlh1 under the splenic capsule, and careful examination of genomic DNA extracted from laser-capture microdissected tumor tissue excluded the presence of an MSI phenotype. Strikingly, these mice exhibited the shortest median survival. We speculate that these mice may have died from lymphomas that arose from oncogenic mechanisms other than MSI, such as chromosomal instability. Alternatively, these mice may have died from general organ failure due to the greater cytotoxicity of azathioprine in *Msh2*^{WT} cells. In support of the latter mechanism are data showing that human *Msh2*$^{+/-}$ lymphoblastoid cells are approximately fourfold more tolerant than wild-type cells to killing by temozolomide, a methylating agent known to involve a DNA mismatch repair–dependent signaling response to DNA damage (47).

Our findings could have important clinical implications for patients receiving azathioprine therapy. *Msh2*$^{-/-}$ mice spontaneously develop lymphomas and display the phenotype of the rare patients with homozygous or biallelic inactivation of DNA mismatch repair genes, including a severely reduced lifespan and increased frequency of hematological malignancies compared with general population (48). We have shown that all azathioprine-induced lymphomas in *Msh2*$^{+/-}$ mice arise from an MSI-driven oncogenic process following inactivation of the *Msh2* wild-type allele, mainly through loss of heterozygosity. Mice with one constitutively inactivated *Msh2* allele are the murine equivalent of

the HNPCC syndrome, one of the most common genetic predispositions to cancer in humans. However, unlike humans who carry a heterozygous mutation in a DNA mismatch repair gene, *Msh2*$^{+/-}$ mice do not spontaneously develop neoplasms with MSI. HNPCC is relatively prevalent, affecting 2%–5% of patients diagnosed with colorectal cancer (49). Given that the lifetime risk of colorectal cancer is approximately 6% in the United States (50), we estimate that HNPCC may affect approximately one of 300–800 individuals in the general population. Moreover, because the evaluated incidence of HNPCC relies on the early age at cancer diagnosis and family history of cancer, it is likely to be underestimated because the penetrance of the syndrome may be largely incomplete and HNPCC may also be characterized by the emergence of late-onset tumors in some patients (51). Finally, lymphomas that developed in azathioprine-treated *Msh2*^{WT} mice did not display MSI, whereas we previously detected MSI in a minority (8%) of lymphomas that developed in a large cohort (n = 111) of non-HNPCC patients treated with azathioprine and/or other immunosuppressants (21). Together, the above observations indicate that azathioprine and, more broadly, the thiopurines constitute only a minor risk factor for the development of tumors with MSI in the general population. However, for individuals who carry mutations in DNA mismatch repair genes, exposure to azathioprine may be an important risk factor for the development of tumors with MSI. Our results could thus have important implications for the use of azathioprine in heterozygous carriers of DNA mismatch repair gene defects. On the basis of our findings, we recommend that more effort should be directed toward identifying possible cases of HNPCC among patients who are frequently prescribed thiopurines, such as transplant patients and patients suffering from inflammatory diseases. In addition, systematic screening for mutations in DNA mismatch repair genes in azathioprine-treated patients who subsequently developed DNA mismatch repair–deficient neoplasms could unmask previously unrecognized cases of HNPCC. Because earlier results by our group showed that MSI-associated lymphoproliferative disorders in transplant patients were usually late onset (22), this possibility should be considered, especially when the tumor is diagnosed long after the immunosuppressive therapy. Consequently, we recommend systematic screening for MSI in lymphomas and other neoplasms that arise in patients treated with thiopurine drugs. This screening could be particularly important because tumors with MSI usually have a different prognosis and sensitivity to chemotherapeutic agents compared with tumors that lack MSI, as has been shown for colorectal carcinomas (52).

To date, the mechanisms through which iatrogenic neoplasms arise in patients who are treated with different drugs in various clinical contexts are largely unknown. Here we show that mouse models can be highly relevant for the investigation of this issue because they can allow the identification of a known cancer pathway in relation to the prescription of a specific drug. Following on from these findings, we recommend that similar studies be carried out to determine whether other cancer-related genes play a role in the development of secondary neoplasms in response to other therapeutic agents. This study has provided further insight into the mechanisms that underlie azathioprine-induced carcinogenesis, including the ability of this drug to induce MSI-driven malignancy in *Msh2*$^{+/-}$ mice. The limitation of this study is that we did not investigate if such observations are specific for thiopurines or whether they could be extended to other frequently prescribed immunosuppressants whose actions are independent of DNA mismatch repair. It is generally considered that MSI tumors are tightly controlled by the host's immune system. Indeed, tumors that display MSI are characterized by a high level of lymphocytic infiltration due to their highly immunogenic nature (53), and it has been shown that aberrant neoantigenic peptides resulting from genes carrying frameshift mutations may elicit an immune response against tumor cells displaying MSI, which could then limit their proliferation (54,55). Further studies analogous to this study involving other frequently prescribed immunosuppressants are required to determine whether a reduction in host immunosurveillance, by itself, plays a role in MSI-driven oncogenesis.

References

1. Allan JM, Rabkin CS. Genetic susceptibility to iatrogenic malignancy. *Pharmacogenomics.* 2005;6(6):615–628.
2. Burchenal JH, Murphy ML, Ellison RR, et al. Clinical evaluation of a new antimetabolite, 6-mercaptopurine, in the treatment of leukemia and allied diseases. *Blood.* 1953;8(11):965–999.
3. Elion GB. The purine path to chemotherapy. *Science.* 1989;244(4900):41–47.
4. Azathioprine. *IARC Monogr.* 1987;26(suppl 7:119.
5. Karran P, Offman J, Bignami M. Human mismatch repair, drug-induced DNA damage, and secondary cancer. *Biochimie.* 2003;85(11):1149–1160.
6. Karran P, Attard N. Thiopurines in current medical practice: molecular mechanisms and contributions to therapy-related cancer. *Nat Rev Cancer.* 2008;8(1):24–36.
7. Schulz TF. Cancer and viral infections in immunocompromised individuals. *Int J Cancer.* 2009;125(8):1755–1763.
8. Hawn MT, Umar A, Carethers JM, et al. Evidence for a connection between the mismatch repair system and the G2 cell cycle checkpoint. *Cancer Res.* 1995;55(17):3721–3725.
9. Offman J, Opelz G, Doehler B, et al. Defective DNA mismatch repair in acute myeloid leukemia/myelodysplastic syndrome after organ transplantation. *Blood.* 2004;104(3):822–828.
10. Borgdorff V, van Hees-Stuivenberg S, Meijers CM, de Wind N. Spontaneous and mutagen-induced loss of DNA mismatch repair in Msh2-heterozygous mammalian cells. *Mutat Res.* 2005;574(1–2):50–57.
11. Karran P, Bignami M. DNA damage tolerance, mismatch repair and genome instability. *Bioessays.* 1994;16(11):833–839.
12. Swann PF, Waters TR, Moulton DC, et al. Role of postreplicative DNA mismatch repair in the cytotoxic action of thioguanine. *Science.* 1996; 273(5278):1109–1111.
13. Waters TR, Swann PF. Cytotoxic mechanism of 6-thioguanine: hMutSalpha, the human mismatch binding heterodimer, binds to DNA containing S6-methylthioguanine. *Biochemistry.* 1997;36(9):2501–2506.
14. Thiopurines Karran P. DNA damage, DNA repair and therapy-related cancer. *Br Med Bull.* 2006. 79–80:153–170.
15. Coulthard S, Hogarth L. The thiopurines: an update. *Invest New Drugs.* 2005;23(6):523–532.
16. Ionov Y, Peinado MA, Malkhosyan S, Shibata D, Perucho M. Ubiquitous somatic mutations in simple repeated sequences reveal a new mechanism for colonic carcinogenesis. *Nature.* 1993;363(6429):558–561.
17. Thibodeau SN, Bren G, Schaid D. Microsatellite instability in cancer of the proximal colon. *Science.* 1993;260(5109):816–819.
18. Peltomaki P, Lothe RA, Aaltonen LA, et al. Microsatellite instability is associated with tumors that characterize the hereditary non-polyposis colorectal carcinoma syndrome. *Cancer Res.* 1993;53(24):5853–5855.
19. Boland CR, Thibodeau SN, Hamilton SR, et al. A National Cancer Institute Workshop on Microsatellite Instability for cancer detection and familial predisposition: development of international criteria for the determination of microsatellite instability in colorectal cancer. *Cancer Res.* 1998;58(22):5248–5257.

20. Casorelli I, Offman J, Mele L, et al. Drug treatment in the development of mismatch repair defective acute leukemia and myelodysplastic syndrome. *DNA Repair (Amst).* 2003;2(5):547–559.
21. Duval A, Raphael M, Brennetot C, et al. The mutator pathway is a feature of immunodeficiency-related lymphomas. *Proc Natl Acad Sci U S A.* 2004;101(14):5002–5007.
22. Borie C, Colas C, Dartigues P, et al. The mechanisms underlying MMR deficiency in immunodeficiency-related non-Hodgkin lymphomas are different from those in other sporadic microsatellite instable neoplasms. *Int J Cancer.* 2009;125(10):2360–2366.
23. Svrcek M, El-Bchiri J, Chalastanis A, et al. Specific clinical and biological features characterize inflammatory bowel disease associated colorectal cancers showing microsatellite instability. *J Clin Oncol.* 2007;25(27):4231–4238.
24. de Wind N, Dekker M, Berns A, Radman M, te Riele H. Inactivation of the mouse Msh2 gene results in mismatch repair deficiency, methylation tolerance, hyperrecombination, and predisposition to cancer. *Cell.* 1995;82(2):321–330.
25. Toft NJ, Winton DJ, Kelly J, et al. Msh2 status modulates both apoptosis and mutation frequency in the murine small intestine. *Proc Natl Acad Sci U S A.* 1999;96(7):3911–3915.
26. Reagan-Shaw S, Nihal M, Ahmad N. Dose translation from animal to human studies revisited. *FASEB J.* 2008;22(3):659–661.
27. Anstey AV, Wakelin S, Reynolds NJ. Guidelines for prescribing azathioprine in dermatology. *Br J Dermatol.* 2004;151(6):1123–1132.
28. Yip JS, Woodward M, Abreu MT, Sparrow MP. How are azathioprine and 6-mercaptopurine dosed by gastroenterologists? Results of a survey of clinical practice. *Inflamm Bowel Dis.* 2008;14(4):514–518.
29. Opelz G, Dohler B. Critical threshold of azathioprine dosage for maintenance immunosuppression in kidney graft recipients. Collaborative Transplant Study. *Transplantation.* 2000;69(5):818–821.
30. Fabre MA, Jones DC, Bunce M, et al. The impact of thiopurine S-methyltransferase polymorphisms on azathioprine dose 1 year after renal transplantation. *Transpl Int.* 2004;17(9):531–539.
31. Cuffari C, Hunt S, Bayless T. Utilisation of erythrocyte 6-thioguanine metabolite levels to optimise azathioprine therapy in patients with inflammatory bowel disease. *Gut.* 2001;48(5):642–646.
32. Jourdan F, Sebbagh N, Comperat E, et al. Tissue microarray technology: validation in colorectal carcinoma and analysis of p53, hMLH1, and hMSH2 immunohistochemical expression. *Virchows Arch.* 2003;443(2):115–121.
33. Duval A, Gayet J, Zhou XP, Iacopetta B, Thomas G, Hamelin R. Frequent frameshift mutations of the TCF-4 gene in colorectal cancers with microsatellite instability. *Cancer Res.* 1999;59(17):4213–4215.
34. Reitmair AH, Redston M, Cai JC, et al. Spontaneous intestinal carcinomas and skin neoplasms in Msh2-deficient mice. *Cancer Res.* 1996;56(16):3842–3849.
35. de Wind N, Dekker M, van Rossum A, van der Valk M, te Riele H. Mouse models for hereditary nonpolyposis colorectal cancer. *Cancer Res.* 1998;58(2):248–255.
36. Isidro G, Veiga I, Matos P, et al. Four novel MSH2/MLH1 gene mutations in portuguese HNPCC families. *Hum Mutat.* 2000;15(1):116.
37. Lowsky R, Magliocco A, Ichinohasama R, et al. MSH2-deficient murine lymphomas harbor insertion/deletion mutations in the transforming growth factor beta receptor type 2 gene and display low not high frequency microsatellite instability. *Blood.* 2000;95(5):1767–1772.
38. Carbonnelle D, Jacquot C, Lanco X, et al. Up-regulation of a novel mRNA (NY-CO-1) involved in the methyl 4-methoxy-3-(3-methyl-2-butenoyl) benzoate (VT1)-induced proliferation arrest of a non-small-cell lung carcinoma cell line (NSCLC-N6). *Int J Cancer.* 2001;92(3):388–397.
39. Bi X, Jones T, Abbasi F, et al. Drosophila caliban, a nuclear export mediator, can function as a tumor suppressor in human lung cancer cells. *Oncogene.* 2005;24(56):8229–8239.
40. Degot S, Le Hir H, Alpy F, et al. Association of the breast cancer protein MLN51 with the exon junction complex via its speckle localizer and RNA binding module. *J Biol Chem.* 2004;279(32):33702–33715.
41. El-Bchiri J, Buhard O, Penard-Lacronique V, Thomas G, Hamelin R, Duval A. Differential nonsense mediated decay of mutated mRNAs in mismatch repair deficient colorectal cancers. *Hum Mol Genet.* 2005;14(16):2435–2442.
42. El-Bchiri J, Guilloux A, Dartigues P, et al. Nonsense-mediated mRNA decay impacts MSI-driven carcinogenesis and anti-tumor immunity in colorectal cancers. *PLoS One.* 2008;3(7):e2583.
43. Hutchinson P, Jose M, Atkins RC, Holdsworth SR. Ex vivo lymphocyte proliferative function is severely inhibited in renal transplant patients on mycophenolate mofetil treatment. *Transpl Immunol.* 2004;13(1):55–61.
44. Fairbanks LD, Bofill M, Ruckemann K, Simmonds HA. Importance of ribonucleotide availability to proliferating T-lymphocytes from healthy humans. Disproportionate expansion of pyrimidine pools and contrasting effects of de novo synthesis inhibitors. *J Biol Chem.* 1995;270(50):29682–29689.
45. Quemeneur L, Gerland LM, Flacher M, Ffrench M, Revillard JP, Genestier L. Differential control of cell cycle, proliferation, and survival of primary T lymphocytes by purine and pyrimidine nucleotides. *J Immunol.* 2003;170(10):4986–4995.
46. Knudson AG Jr. Mutation and cancer: statistical study of retinoblastoma. *Proc Natl Acad Sci U S A.* 1971;68(4):820–823.
47. Marra G, D'Atri S, Corti C, et al. Tolerance of human MSH2+/- lymphoblastoid cells to the methylating agent temozolomide. *Proc Natl Acad Sci U S A.* 2001;98(13):7164–7169.
48. Felton KE, Gilchrist DM, Andrew SE. Constitutive deficiency in DNA mismatch repair. *Clin Genet.* 2007;71(6):483–498.
49. Hampel H, Frankel WL, Martin E, et al. Feasibility of screening for lynch syndrome among patients with colorectal cancer. *J Clin Oncol.* 2008;26(35):5783–5788.
50. Levin KE, Dozois RR. Epidemiology of large bowel cancer. *World J Surg.* 1991;15(5):562–567.
51. Jenkins MA, Baglietto L, Dowty JG, et al. Cancer risks for mismatch repair gene mutation carriers: a population-based early onset case-family study. *Clin Gastroenterol Hepatol.* 2006;4(4):489–498.
52. Popat S, Hubner R, Houlston RS. Systematic review of microsatellite instability and colorectal cancer prognosis. *J Clin Oncol.* 2005;23(3):609–618.
53. Smyrk TC, Watson P, Kaul K, Lynch HT. Tumor-infiltrating lymphocytes are a marker for microsatellite instability in colorectal carcinoma. *Cancer.* 2001;91(12):2417–2422.
54. Saeterdal I, Bjorheim J, Lislerud K, et al. Frameshift-mutation-derived peptides as tumor-specific antigens in inherited and spontaneous colorectal cancer. *Proc Natl Acad Sci U S A.* 2001;98(23):13255–13260.
55. Ishikawa T, Fujita T, Suzuki Y, et al. Tumor-specific immunological recognition of frameshift-mutated peptides in colon cancer with microsatellite instability. *Cancer Res.* 2003;63(17):5564–5572.

Funding

This work was partly supported by grants to Alex Duval from the Association pour la Recherche contre le Cancer (ARC 1041) and to Martine Muleris from the GEFLUC (Groupement des Entreprises Françaises dans la LUtte contre le Cancer). Alexandra Chalastanis is a recipient of an MESR fellowship (Ministère de l'Enseignement Supérieur et de la Recherche).

Notes

The authors wish to thank Dominique Wendum for providing access to the laser-capture microdissection platform (Institut de Recherche en Santé Saint-Antoine - IFR 65) and Agathe Guilloux (Laboratoire de statistique théorique et appliquée, UPMC, Paris) for expert assistance in statistical analyses. The funders did not have any role in the in the design of the study, analysis or interpretation of the data, the writing of the manuscript, or the decision to submit the manuscript for publication.

Affiliations of authors: INSERM, UMRS 938, Paris, France (AC, MS, OB, J-FF, AD, MM); UPMC-Paris 6, France (AC, MS, OB, SD, J-FF, AD, MM); INSERM, U985, Paris, France (VP-L); Université Paris Descartes, Paris, France (VP-L); AP-HP Hôpital Saint-Antoine, Service d'Anatomie Pathologique, Paris, France (MS, BF, J-FF); Human Histology Laboratory, Faculty of Medicine (VD) and Laboratory of Animal Histology and Embryology, Faculty of Veterinary Medicine, University of Liège, Liège, Belgium (NA); IFR 65, Paris, France (SD, IR); CEPH, Paris, France (ET); Division of Molecular Biology, The Netherlands Cancer Institute, Amsterdam, the Netherlands (HtR).